99mTc-Glucarate for assessment of paclitaxel therapy in human ovarian cancer in mice

Hossein Sadeghi [1], Najmeh Rahmanian [1], Fereshteh Talebpour Amiri [2], Hossein Amirfakhrian [1], Seyed Mohammad Abedi [3], Seyed Jalal Hosseinimehr [1]*

[1] Department of Radiopharmacy, Faculty of Pharmacy, Mazandaran University of Medical Sciences, Sari, Iran
[2] Department of Anatomy, Faculty of Medicine, Molecular and Cell Biology Research Center, Mazandaran University of Medical Sciences, Sari, Iran
[3] Department of Radiology, Faculty of Medicine, Mazandaran University of Medical Sciences, Sari, Iran

ARTICLE INFO	ABSTRACT
	Objectives: The monitoring of cancer treatment response to chemotherapy is considered an essential strategy for follow-up of patients. The aim of this study was to evaluate the use of 99mTc-glucarate as a radiotracer for *in vivo* quantification and visualization of necrotic area and therapeutic effect of paclitaxel in ovarian cancer xenografted nude mice. *Materials and Methods:* After implantation of human ovarian cancer (SKOV-3) in nude mice, tumor xenografted mice were enrolled in two groups as control and treatment (paclitaxel) groups. 99mTc-glucarate uptakes were quantified in tumors of control and treatment groups and also tumor imaging was performed with a gamma camera. The necrotic and viable areas of tumor and tumoral masses were evaluated through histopathological and macroscopic observations, respectively. *Results:* 99mTc-glucarate uptake in tumor of treatment group was higher than control group. 99mTc-glucarate uptake in ovarian tumor was clearly visualized with gamma imaging in both groups, but paclitaxel treated group showed higher radioactive uptake than control mice. The necrotic area in tumoral mass of mice treated with paclitaxel was confirmed by histopathological observations. *Conclusion:* 99mTc-glucarate is an effective radiotracer for evaluation and monitoring of tumor necrosis caused by chemotherapy, and it may be helpful for therapy monitoring in patients with cancer.

Introduction

Ovarian cancer is the one of the most common cancer of the female reproductive system (1, 2). Despite surgery and chemotherapy for treatment of patients with advanced ovarian cancer, five-year survival rates were reported to be 36% and 8% for stage III and stage IV, respectively (1, 2). Chemotherapy is one of the most common strategies for cancer treatment. Anti-cancer agents inhibit the division of rapidly growing cells, which is a characteristic of the cancerous cells. Paclitaxel (Taxol®) is widely used as a chemotherapy agent for the treatment of various cancers such as metastatic breast cancer, advanced ovarian cancer, and non-small cell lung cancer (3, 4).

The tubular/microtubular system is suggested as an intercellular target for paclitaxel (5). But, the exact mechanism of the cytotoxicity of paclitaxel against tumor cells is still under investigations. Yeung *et al.* proposed that paclitaxel-induced cell death occurs through two modes, apoptosis at low concentra-

tion and necrosis at high concentration (6).

Paclitaxel induces necrosis and apoptosis in human endothelial cells (7). Paclitaxel is used an effective anti-neoplastic agent on various cancers, especially ovarian cancer (3). Paclitaxel causes necrotic area in ovarian tumor xenografts in animal (8). Current standard diagnostic techniques for staging of ovarian cancer are measuring the level of CA-125 (Mucin 16) in serum and ultrasonography (9).

Because of the deficiency of medical diagnostics tools in early detection of disease, most patients with ovarian cancer have advanced disease at the time of diagnosis (10). For patient who progresses on cancer treatment, the efficacy of paclitaxel should be monitored during the therapy. For this reason, for planning and following-up of treatment in many cancers, 18F-fluorodeoxyglucose (18F-FDG) as positron emission tomography (PET) is used for monitoring of cancer treatment; it has sensitivity of 91% and specificity of 88% (11).

Corresponding author: Seyed Jalal Hosseinimehr. Department of Radiopharmacy, Faculty of Pharmacy, Mazandaran University of Medical Sciences, Sari, Iran. Tel: +98-11-33261244. email: sjhosseinim@yahoo.com; sjhosseinim@mazums.ac.ir

Due to high cost and low accessibility in many areas of the world, the use of ^{18}F-FDG is limited; therefore, it is necessary to find a substitute technique and proper radiopharmaceutical agent instead of ^{18}F-FDG (12). ^{99m}Tc-glucarate has been used as a radiopharmaceutical agent for imaging of myocardial infarction (13, 14), acute cerebral injury (15) and in tumors (16-18). Accumulation of ^{99m}Tc-glucarate in normal and apoptotic cells is less than necrotic cells (19). Glucarate is a metabolite of D-glucuronic acid as a natural product, which has low molecular weight with six-carbon dicarboxylic acid structure that could be labeled with [99m]Tc (20). ^{99m}Tc-glucarate could be used in single-photon emission computed tomography (SPECT) that is more cost-effective and accessible than ^{18}F-FDG (12). The aim of this study was to evaluate the use of ^{99m}Tc-glucarate in the assessment of necrotic area and therapeutic effect of paclitaxel in ovarian cancer xenografted nude mice. The results of ^{99m}Tc-glucarate uptake and tumor imaging were compared with pathological data.

Materials and Methods

Glucaric acid (D-saccharic acid potassium salt) was purchased from Sigma (USA). Paclitaxel was purchased from Sobhan Oncology Company (Rasht, Iran). The [99m]TcO$_4$Na was eluted from a [99]Mo/^{99m}Tc radionuclide generator (Parsisotope, Tehran, Iran). Radiochemical purity was assayed with instant thin layer chromatography (ITLC). The distribution of radio-activity on the ITLC strips was quantized using a Lablogic mini-scan TLC scanner and analyzed with Laura image analysis software (Sheffield, UK). Radioactivity in the samples was measured using a NaI(Tl) gamma detector (Delshid, Iran).

Preparation of ^{99m}Tc-glucarate

[99m]Tc-glucarate was prepared according to a method that was previously published by Babbar and Sharma with minor modifications (21). The single-vial compositions were 12 mg mono potassium glucarate, 0.1 mg SnCl$_2$.2H$_2$O, and sodium bicarbonate in saline. ^{99m}Tc-glucarate was obtained after adding about 278 MBq of [99m]TcO$_4$Na to vial (pH 8). The mixture was shaken for one minute and allowed to react at room temperature for 20 min. Then, 200 μl HCl (0.1 N) was added to mixture for adjusting pH to 7-7.5. Radiochemical purity (RCP) was determined by ITLC strips developed in 0.9% saline and methyl ethyl ketone (MEK). In the ITLC strip developed by saline, ^{99m}Tc-colloid remained at the origin while ^{99m}Tc-glucarate and free ^{99m}Tc migrated at the solvent front. In the ITLC strip developed by MEK, ^{99m}Tc-glucarate remained at the origin while the free ^{99m}Tc was at the solvent front.

Tumor model

All animal experiments were approved by Research and Ethical Committee of Mazandaran University of Medical Sciences, Sari, Iran. The study was performed on female nude mice bearing human ovarian tumor (SKOV-3). SKOV-3 cell line was purchased from the Pasture Institute of Iran (Tehran, Iran) and cultured in Dulbecco's Modified Eagle's medium (DMEM) medium supplemented with 10% fetal bovine serum (FBS) and penicillin–streptomycin (Gibco, Grand Island, NY) at 37 °C in a humidified environment and 5% CO$_2$. Female nude mice (3 to 5-week-old, 14-18 g) (Institute Pasteur, North Branch, Amol, Iran) were inoculated subcutaneously in the right hind leg with SKOV-3 cells (1×10^7) in 100 μl of complete DMEM. After 48 hrs of tumor implantation, all the tumor-bearing mice were divided randomly into two groups as control and treatment groups. As soon as the tumor was palpable (0.25 mm^3), the tumor measuring was started and it was stated as day 1. Paclitaxel treatment was started when the tumor volume of the mice reached 200–250 mm^3 (on day 14 after tumor inoculation). Tumor sizes were measured every day to evaluate the antitumor efficacy of paclitaxel. Tumor-bearing mice were received intraperitoneally paclitaxel (40 mg/kg total dose over 2 duration or 20 mg/kg drug on a q7d×2 schedule). Control animals were received normal saline in same manner to treatment group.

Tumor measurements were made using a vernier caliper while mice were conscious and were calculated according to formula as a standard practice (tumor volume = $xy^2/2$). The length (x) is considered to be equivalent to the greatest longitudinal diameter and this considered to be equivalent to the greatest transverse diameter (22, 23).

Biodistribution

[99m]Tc-glucarate was injected into the tail vein of both groups (treatment and control) of mice bearing tumors. The mice were sacrificed at 30 min post-injection. Blood and samples from the lung, liver, spleen, salivary gland, stomach, kidney, muscle, bone and tumor were dissected and weighed, and their radioactivities were measured. The tissue uptake values were calculated as percent of injected dose per gram tissue (%ID/g).
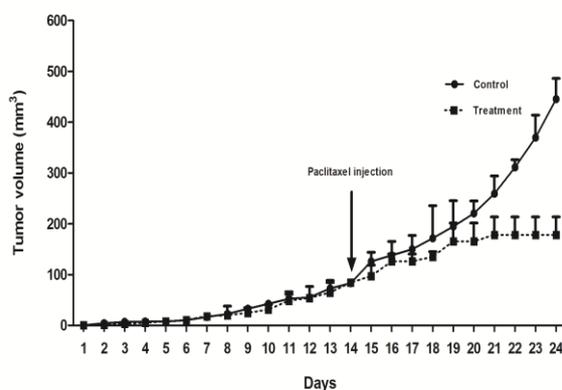

Figure 1. Tumor size changes in nude mice bearing human ovarian tumor in control group and following injection of paclitaxel treatment group (n = 4)

Tumor gamma camera imaging

Planar imaging studies were carried out with anesthetized SKOV-3 tumor-bearing mice to acquire a visual confirmation of the tumor uptake. Images were acquired at 30 min post-injection of 99mTc-glucarate using an E-CAM dual head (Siemens Medical Solutions, Germany) equipped with a low energy high-resolution collimator.

Histological analysis

The tumoral specimens were fixed in 10% formalin, processed routinely, embedded in paraffin, sectioned at 5 μm, deparaffinized and stained with hematoxylin–eosin (H&E). Slides from each group were investigated by an observer blinded to the treatments. An Olympus microscope at × 20 magnifications was used to evaluate the effect of paclitaxel on cell density, necrosis, fibrosis and neovascularization.

Statistical analysis

Data were statistically analyzed using Excel software (Microsoft office, USA) using unpaired t-test. For all tests, *P*-values less than 0.05 were considered significant.

Results

Preparation of 99mTc-glucarate

99mTc-glucarate was obtained with a radiochemical purity more than 98% (n = 10) (Supplementary Figure S1 and S2). The stability of 99mTc-glucarate was assessed in normal saline and it was 98% ± 0.03 up to 4 hr (Supplementary Figure S3).

Tumor growth and paclitaxel therapy

Nude mice bearing ovarian tumor were injected with paclitaxel on day 14 after tumor sizes were 200 – 250 mm^3 (Figure 1). Tumor sizes were increased rapidly in control group, while paclitaxel treatment resulted in tumor growth inhibition (*P*< 0.05). At the end of 11 day of paclitaxel therapy, 99mTc-glucarate was injected and animal biodistribution was conducted. At this time, the result of tumor growth experiment showed that paclitaxel inhibited tumor growth in animal.
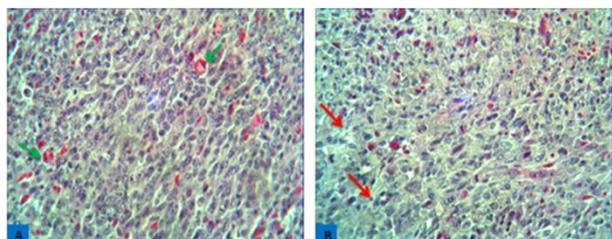

Figure 2. Histopathological findings of the effect of paclitaxel on ovarian cancer tissue (SKOV-3). (A) Control group (B) treatment with paclitaxel (20 mg/kg/week) for 11 days. Histopathological analysis of tumoral masses treated with paclitaxel showed increase in necrotic and fibrotic areas versus control. Sign red star shows necrosis of tumoral mass. Sign green star shows the neovascularization (H & E. × 400). Scale bar = 100 μm
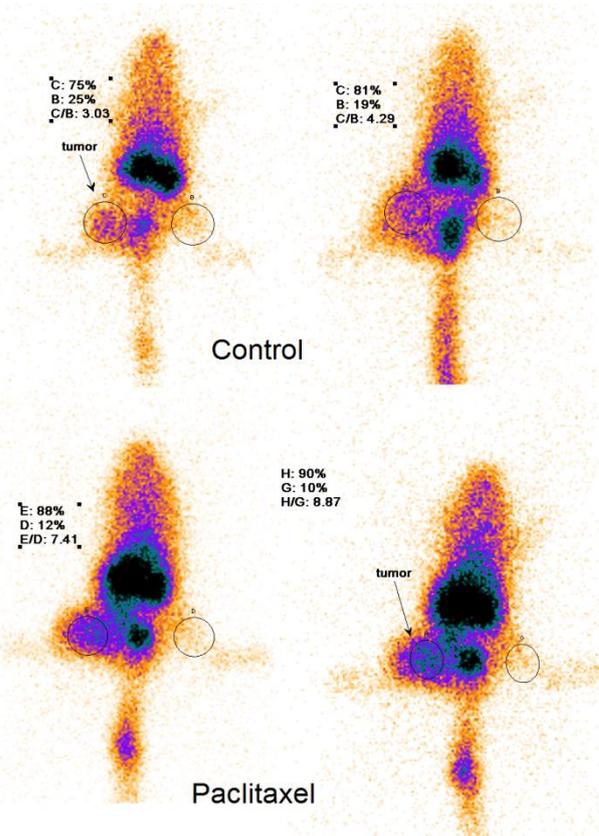

Figure 3. Whole body images of mice bearing human ovarian cancer were injected 99mTc-glucarate. Human ovarian cancer xenografted mice are control and paclitaxel treated animals. Tumor-background ratio is about 2-fold higher in paclitaxel treated mice as compared to control mice

Biodistribution of 99mTc-glucarate

Biodistribution data in nude mice bearing ovarian tumor at 30 min post-injection of 99mTc-glucarate are presented in Table 1. The tumor uptake of 99mTc-glucarate was higher than muscle uptake in both groups of control and paclitaxel treatment. Tumor uptake of the 99mTc-glucarate was higher in necrotic tumors (4.71 ± 0.9% ID/g) than in control tumors (3.05 ± 0.4% ID/g) (*P* <0.05). The tumor-blood ratio was 0.7 ± 0.1% ID/g and 0.93 ± 0.4% ID/g in control and treatment groups, respectively. The tumor-muscle ratio was 2.71 ± 0.3% ID/g and 3.45 ± 0.4% ID/g in control and treatment groups, respectively. The highest normal organ uptake of radioactivity was observed in the kidneys that exhibited the main excretory route of 99mTc-glucarate is renal system, also low radioactivities were observed in liver and intestines.

Macroscopic observation of tumors

In macroscopic study, in all nude mice, tumoral mass developed for 24 days after ovarian cancer (SKOV-3) implantation. When paclitaxel administration was started, tumoral tissue volume in the treatment group showed a decrease of 2.5 fold at end of experiment (Figure 1).

Table 1. Biodistribution of 99mTc-glucarate in female nude mice bearing human ovarian SKOV-3 tumors at 0.5 hr post-injection

Tissue	Control		Treatment (paclitaxel)	
	%ID/g	Tumor/organ#	%ID/g	Tumor/organ
Blood	4.47 ± 1.00	0.70	5.90 ± 2.86	0.93
Heart	1.36 ± 0.33	2.38	2.83 ± 0.75	1.75
Lung	3.69 ± 0.80	0.88	4.45 ± 2.01	1.24
Salivary glands & Thyroid	1.99 ± 0.04	1.53	3.05 ± 1.39	1.77
Liver	2.94 ± 0.71	1.12	4.43 ± 0.46	1.08
Spleen	1.03 ± 0.27	3.06	1.94 ± 0.18	2.45
Kidney	49.22 ± 7.77	0.06	59.85 ± 14.06	0.08
Stomach	1.39 ± 0.25	2.27	2.32 ± 0.66	2.21
Muscle	1.14 ± 0.23	2.71	1.38 ± 0.17	3.42*
Bone	2.09 ± 1.25	1.36	2.29 ± 0.79	2.24
Intestine	3.29 ± 0.26	0.93	4.66 ± 0.75	1.01
Tumor	3.05 ± 0.47		4.71 ± 0.96*	

Each value is the mean ± SD for four mice.*Significant difference between control and paclitaxel therapy, $P<0.05$. #Tumor/organ means the ratios of tumor per each tissue as tumor/blood, tumor/heart, tumor/lung, etc.

In the treated group, tumoral masses seemed soft tissues that were easily separated from the surrounding tissue. While in the control group, tumoral specimens had a firm consistency and infiltrated into the muscle adjacent to the site of ovarian cancer cell implanted. Tumoral tissue completely attached to the muscle and separating the tumoral mass from the surrounding tissue was difficult. It was clear that paclitaxel was able to inhibit the tumor metastasis of ovarian cancer to surrounding tissue. So, treated group had less severity of metastasized ovarian cancer as compared to the control group.

Histopathological findings

Cancer tissue grew actively in the control group. In microscopic study, multinucleate and high cellularity of ovarian cancer was observed in the control group. Administration of paclitaxel induced the necrotic and fibrotic areas with inhibition of angiogenesis in cancer tissue. Paclitaxel could suppress ovarian tumor growth and inhibit the neovascularization and cell proliferation in tumoral mass. The histopathological findings showed about 20-30% necrosis in tumor samples in paclitaxel treated mice (Figure 2).

Tumor imaging

The tumor imaging of female nude mice bearing tumor was evaluated with SPECT at 30 min post-injection of 99mTc-glucarate. The uptake of 99mTc-glucarate was observed in tumors of control and paclitaxel treated mice (Figure 3).

Tumor can be observed in SPECT scan in control and treated mice; however, tumor visualization in treatment group was more than control mice. The radioactivity uptakes were measured as tumor to muscle ratios in control and paclitaxel treated mice. These ratios were 3.66 and 8.14 for control and anti-cancer treated mice, respectively. Imaging finding showed higher tumor to muscle ratio (2 fold) than biodistribution data (1.3 fold) in control and paclitaxel treated mice.

Discussion

The therapeutic strategy in induction of necrotic pathways converges to achieve a more effective treatment of cancer. Evaluation of necrosis seems to be important for monitoring cancer treatment efficacy in patients. Non-invasive molecular imaging techniques, such as 18F-FDG-PET have become an essential imaging tool for the assessment of ovarian cancer treatment (24, 25). 18F-FDG-PET was applied for determination of treatment response in a pre-clinical mouse model of human ovarian cancer xenografts in mice (A2780) treated with carboplatin and paclitaxel. 18F-FDG uptake was lower (about 1.3 fold) in the anti-cancers treatment group as compared to the control group (26). However, the use of PET is limited due to its high price and unavailability in some areas (12). We showed that 99mTc-glucarate as a SPECT imaging agent could be used for *in vivo* imaging and evaluation of necrotic cells in ovarian tumor. 99mTc-glucarate has been used as tumor imaging agent in malignancies of the chest, head and neck, and breast (16-18, 27-30) and lately evaluation of necrotic area in NSCLC tumor (31). 99mTc-glucarate binds to exposed histones in necrotic cells (14, 30, 32). It has been shown that tumors with higher amount of necrosis have higher 99mTc-glucarate uptake than viable cells (17, 18, 28-30). Paclitaxel treatment markedly decreased 18F-FDG uptake in human ovarian cancer xenografts in mice (A2780). 18F-FGD uptake is associated with glucose uptake that is dependent to cell survival and proliferation (25, 26). In our study, 99mTc-glucarate uptake was increased in tumor of paclitaxel treated mice with highly degree of necrosis. Since necrotic cells are unable to uptake glucose, 99mTc-glucarate is not mediated by glucose uptake in necrotic cells and other mechanisms are involved in the 99mTc-glucarate uptake in necrotic cells. Increased uptake of 99mTc-glucarate in necrotic cells could be due to the loss of membrane integrity caused by necrosis, which leads to enhance the penetration into the intracellular space,

while no membrane damage occurs in viable cells and ⁹⁹ᵐTc-glucarate has no direct contact with histones. For this reason, the uptake of ⁹⁹ᵐTc-glucarate varies between necrotic and viable cells (30). Although the exact mechanism of ⁹⁹ᵐTc-glucarate localization is not understood, it is likely that negatively charged ⁹⁹ᵐTc-glucarate is attracted to histones and other positively charged proteins. ⁹⁹ᵐTc-glucarate based on the specific chemical properties of diffusion can be actively or passively transported into cells (14, 15, 27, 30).

In our study, ⁹⁹ᵐTc-glucarate represents appropriate characteristics with low accumulation in non-tumor soft tissue except in its excretion organs. The tumor uptake of ⁹⁹ᵐTc-glucarate in treatment group was 4.71 ± 0.96 ID/g% that was 1.54 fold higher than in control group (3.05% ± 0.47 ID/g %). In our study, the mean tumor to-muscle ratio for ⁹⁹ᵐTc-glucarate was 3.42±0.4 and 2.71±0.3 in treatment and control groups, respectively. In other reported study, in U937 leukemia bearing mice, the uptake of ⁹⁹ᵐTc-glucarate in necrotic tumor was 1.71±0.2 ID/g% that was higher than non-treated control tumor 0.61±0.11 ID/g %, and the tumor-muscle ratio was 5.76 ± 0.35 and 2.5 ± 0.4 in the necrotic and control groups, respectively (30). The higher tumor to muscle ratio and uptake for necrotic U937 tumors could be due to a larger percent necrosis per volume and the time of sacrificing animal after injection. However, this study did not present any SPECT imaging of tumor in control and treated nude mice (30). In our study, the locations of ovarian tumors in the mice thigh were observed in the SPECT images in both groups that were injected with ⁹⁹ᵐTc-glucarate, but tumor image was clearer in paclitaxel treated animal than untreated animal.

Conclusion

Inhibiting the growth and proliferation of cancer has become one of the effective strategies in cancer chemotherapy. We examined the use of ⁹⁹ᵐTc-glucarate as a radiotracer for assessment of paclitaxel-induced tumor cell necrosis in nude mice. In paclitaxel -treated group, it was observed more necrotic cells than in the control group. The results showed that the uptake of ⁹⁹ᵐTc-glucarate was higher in necrotic area that was caused by paclitaxel. Morphologic findings including inhibition of neovascularization, necrotic area and cell proliferation were more in paclitaxel-treated group as compared to control group. Histopathological examinations confirmed *in vivo* imaging and biodistribution with ⁹⁹ᵐTc-glucarate that was able to distinguish necrotic cells from viable cells.

Acknowledgment

Conflict of interest

The authors declared no potential conflict of interest with respect to authorship, and/or publication of this study.

References

1. Tortolero-Luna G, Mitchell MF. The epidemiology of ovarian cancer. J Cell Biochem Suppl 1995; 23:200-207.
2. Baldwin LA, Huang B, Miller RW, Tucker T, Goodrich ST, Podzielinski I, *et al.* Ten-year relative survival for epithelial ovarian cancer. Obstet Gynecol 2012; 120:612-618.
3. Muggia FM, Braly PS, Brady MF, Sutton G, Niemann TH, Lentz SL, *et al.* Phase III randomized study of cisplatin versus paclitaxel versus cisplatin and paclitaxel in patients with suboptimal stage III or IV ovarian cancer: a gynecologic oncology group study. J Clin Oncol 2000; 18:106-115.
4. Zhang D, Yang R, Wang S, Dong Z. Paclitaxel: new uses for an old drug. Drug Des Devel Ther 2014; 8:279-284.
5. Kampan NC, Madondo MT, McNally OM, Quinn M, Plebanski M. Paclitaxel and its evolving role in the management of ovarian cancer. Biomed Res Int 2015; 2015:413076.
6. Yeung TK, Germond C, Chen X, Wang Z. The mode of action of taxol: apoptosis at low concentration and necrosis at high concentration. Biochem Biophys Res Commun 1999; 263:398-404.
7. Mailloux A, Grenet K, Bruneel A, Beneteau-Burnat B, Vaubourdolle M, Baudin B. Anticancer drugs induce necrosis of human endothelial cells involving both oncosis and apoptosis. Eur J Cell Biol 2001; 80:442-449.
8. Wu Y, Chu Q, Tan S, Zhuang X, Bao Y, Wu T, *et al.* D-alpha-tocopherol polyethylene glycol succinate-based derivative nanoparticles as a novel carrier for paclitaxel delivery. Int J Nanomedicine 2015; 10:5219-5235.
9. Neesham D. Ovarian cancer screening. Aust Fam Physician 2007; 36:126-128.
10. Kumar S, Mahdi H, Bryant C, Shah JP, Garg G, Munkarah A. Clinical trials and progress with paclitaxel in ovarian cancer. Int J Womens Health 2010; 2:411-427.
11. Iyer VR, Lee SI. MRI, CT, and PET/CT for ovarian cancer detection and adnexal lesion characterization. AJR Am J Roentgenol 2010; 194:311-321.
12. Berger M, Gould MK, Barnett PG. The cost of positron emission tomography in six United States Veterans Affairs hospitals and two academic medical centers. AJR Am J Roentgenol 2003; 181:359-365.
13. Arteaga de Murphy C, Ferro-Flores G, Villanueva-Sanchez O, Murphy-Stack E, Pedraza-Lopez M, Melendez-Alafort L, *et al.* ⁹⁹ᵐTc-glucarate for detection of isoproterenol-induced myocardial infarction in rats. Int J Pharm 2002; 233:29-34.
14. Khaw B-A, Nakazawa A, O'donnell SM, Pak K-Y, Narula J. Avidity of technetium 99m glucarate for the necrotic myocardium: *in vivo* and *in vitro* assessment. J Nucl Cardiol 1997; 4:283-290.
15. Yaoita H, Uehara T, Brownell AL, Rabito CA, Ahmad M, Khaw BA, *et al.* Localization of technetium-99m-glucarate in zones of acute cerebral injury. J Nucl Med 1991; 32:272-278.
16. Petrov AD, Narula J, Nakazawa A, Pak KY, Khaw BA. Targeting human breast tumour in xeno-grafted SCID mice with 99Tcm-glucarate. Nucl Med Commun 1997; 18:241-251.
17. Gambini JP, Cabral P, Santander G, Canepa J, Andruskevicius P, Piuma L, *et al.* ⁹⁹ᵐ Tc-Glucarate as a potential novel tracer of lung cancer lesions. Alasbimn J 2006; 9.

18. Gambini JP, Nuñez M, Cabral P, Lafferranderie M, Noble J, Corchs E*, et al.* Evaluation of patients with head and neck cancer by means of ⁹⁹ᵐTc-glucarate. J Nucl Med Technol 2009; 37:229-232.

19. Choudhury PS, Savio E, Solanki KK, Alonso O, Gupta A, Gambini JP*, et al.* ⁹⁹ᵐTc glucarate as a potential radiopharmaceutical agent for assessment of tumor viability: from bench to the bed side. World J Nucl Med 2012; 11:47-56.

20. Ballinger JR, Proulx A, Ruddy TD. Stable kit formulation of technetium-99m glucarate. Int J Radiat Appl Instrum A 1991; 42:405-406.

21. Babbar A, Sharma R. Formulation of lyophilized cold kit for instant preparation of ⁹⁹ᵐTc-glucarate and its scintigraphic evaluation in experimental models of infarction. Indian J Pharmacol 2003; 35:13-20.

22. Tomayko MM, Reynolds CP. Determination of subcutaneous tumor size in athymic (nude) mice. Cancer Chemother Pharmacol 1989; 24:148-154.

23. Euhus DM, Hudd C, LaRegina MC, Johnson FE. Tumor measurement in the nude mouse. J Surg Oncol 1986; 31:229-234.

24. Prakash P, Cronin CG, Blake MA. Role of PET/CT in ovarian cancer. AJR Am J Roentgenol 2010; 194:W464-470.

25. Abedi SM, Mardanshahi A, Shahhosseini R, Hosseinimehr SJ. Nuclear medicine for imaging of epithelial ovarian cancer. Future Oncol 2016; 12:1165-1177.

26. Munk Jensen M, Erichsen KD, Bjorkling F, Madsen J, Jensen PB, Sehested M*, et al.* Imaging of treatment response to the combination of carboplatin and paclitaxel in human ovarian cancer xenograft tumors in mice using FDG and FLT PET. PLoS One 2013; 8:e85126.

27. Ballinger JR, Hsue V, Rauth AM. Accumulation of technetium-99m glucarate: *in vitro* cell cultures and *in vivo* tumour models. Nucl Med Commun 2003; 24:597-606.

28. Pak K, Nedelman M, Daddona P. Visualization of experimental tumor model: application of a new Tc-99m-labeled compound. J Nucl Med 1989; 30:906.

29. Liu Z, Stevenson GD, Barrett HH, Kastis GA, Bettan M, Furenlid LR*, et al.* ⁹⁹ᵐTc glucarate high-resolution imaging of drug sensitive and drug resistant human breast cancer xenografts in SCID mice. Nucl Med Commun 2004; 25:711.

30. Perek N, Sabido O, Le Jeune N, Prevot N, Vergnon J-M, Clotagatide A*, et al.* Could ⁹⁹ᵐTc-glucarate be used to evaluate tumour necrosis? Eu J Nucl Med Mol Imaging 2008; 35:1290-1298.

31. Meng L, Xiu Y, Li Y, Xu X, Li S, Li X*, et al.* Investigations of ⁹⁹ᵐTc-labeled glucarate as a SPECT radiotracer for non-small cell lung cancer (NSCLC) and potential tumor uptake mechanism. Nucl Med Biol 2015; 42:608-613.

32. Narula J, Petrov A, Pak K-Y, Lister BC, Khaw B-A. Very early noninvasive detection of acute experimental nonreperfused myocardial infarction with ⁹⁹ᵐTc-labeled glucarate. Circulation 1997; 95:1577-1584.